Numerical modelling of the localized fluidization in a saturated granular medium using the coupled method DEM-PFV

Marcella Toraldo
University of the study of Salerno, Italy
CNRS, 3SR, F-38000 Grenoble, France
m.toraldo@studenti.unisa.it - marcella.toraldo@3sr-grenoble.fr

Bruno Chareyre, Luc Sibille
Université Grenoble Alpes, 3SR, F-38000 Grenoble, France
CNRS, 3SR, F-38000 Grenoble, France
Bruno.chareyre@3sr-grenoble.fr luc.sibille@3sr-grenoble.fr

ABSTRACT

We present the numerical results of the progressive fluidization of a saturated granular medium under the effect of a localized upward flow injected from its base. The numerical model used, is based on the coupling between a discrete element model (DEM) for the solid phase and a finite volume method defined at pore scale (PFV) to solve the interstitial fluid flow. By simulating an increase of the injected flux, different regimes are successively observed in the sample: a static bed regime, a dilatation one, a fluidized cavity (that does not open op to the top surface of the granular bed), and finally the fluidization of the total height of the granular specimen inside a fluidized chimney.

INTRODUCTION

The purpose of this study is to simulate numerically the localized fluidization in a saturated granular medium using the coupled method DEM-PFV implemented in YADE code. The numerical model DEM-PFV (Catalano *et al.*, 2014; Sari *et al.*, 2011; Tong *et al.*, 2012), is a micro-hydromechanical model for granular materials that combines the discrete element method for the modelling of the solid phase and a pore-scale finite volume formulation for the flow of an incompressible pore fluid. The numerical results of the progressive development of a fluidized zone, under the effect of a localized upward flow injected at the bottom of the bed, are presented in this paper. Gradually, increasing the injected flux, different regimes are successively observed in the sample: static bed, dilatation, fluidized cavity that doesn't open up to the top surface of the granular bed, and finally fluidization of the total height of the granular specimen inside a fluidized chimney. The simulations are conducted by increasing the injected flux by steps and computing, in the simulation time, values of excess of pressure at the injection point, height of the fluidized zone and height of the specimen. The possibility to represent the results in terms of dimensionless parameters has been investigated by performing simulations with samples constituted with different particle sizes. The two dimensionless graphs are obtained. The first shows the evolution of the normalized excess of pressure with the normalized flux and permits to evaluate the ranges of normalized values of flux for which the different regimes occur. The second shows the evolution of the normalized height of the cavity with the normalized flux and allows to compare the numerical results obtained with some previous experimental results from the literature.

THE SIMULATION

Characteristics of the sample

The sample of dimensions 0.60×0.32×0.10 m (width × height × depth) is constituted by 2000 spherical particles with a mean radius of 0.01125 m, representing the solid phase (Figure 1). All the geometrical and mechanical characteristics of the specimen are reported in the Table 1.

Table 1. Geometrical and mechanical characteristics of the sample

Characteristics of the sample		
Width (w)	[m]	0.60
Height (H_0)	[m]	0.32
Depth (d)	[m]	0.10
Spheres nb.	[-]	2000
Mean radius (r_m)	[m]	0.01125
Porosity (n)	[-]	0.38
Density of the solid phase (ρ_s)	[kg/m^3]	2600
Dynamic viscosity (μ)	[Pa.s]	0.01
Contact friction	[°]	10
Normal contact stiffness ($k_n/2r_m$)	[Pa]	400000
Ratio shear/normal stiffness (k_s/k_n)	[-]	0.5

With respect to the boundary conditions imposed, the sample is constrained only on the bottom edge and not on the top. Periodic conditions are imposed on vertical sides for the particles and for the fluid. It means that, under the action of the flow, the particles at the top of the sample are free to move and those going out from one of the vertical face of the box, come back into the opposite face. This saturated sample is used to investigate, at pore scale, the effects of the fluidization resulting of the injection of an upward flux at the middle of the bottom face of the specimen (Figure 1). In particular, excess of pressure at the injection point, height of the fluidized zone, and height of the specimen are numerically determined in the simulation time from the imposed values of flux.

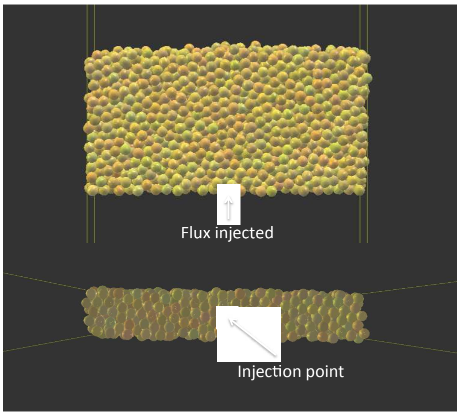

Figure 1. Injection point - the upward flux is injected in the middle of the bottom of the sample

UPWARD INJECTED FLUX

The simulations are conducted increasing the upward injected flux from an initial value of 0.0001 m^3/s, till 0.0261 m^3/s with increments of $0.001m^3/s$ (27 steps). The Figure 2 shows the evolution of the imposed flux (q) and of the computed excess of pressure (p) at the injection point. The excess pressure is given by the difference between the total pressure (p^{tot}) and the hydrostatic pressure: $p = p^{tot} - \rho \cdot g \cdot z$. Each step needs of a large number of iterations depending on the flow rate value in order to reach an established state of the sample. For low values of injected flux, the pressure presents a peak just after the increase of the injected flux but reaches quickly a constant value considered as the established regime. However for larger values of injected flux the pressure needs more time to reaches an established regime. Therefore, the larger the flux is, the higher the number of iterations is to reach an establish regime and to characterize the sample behaviour for this flux.

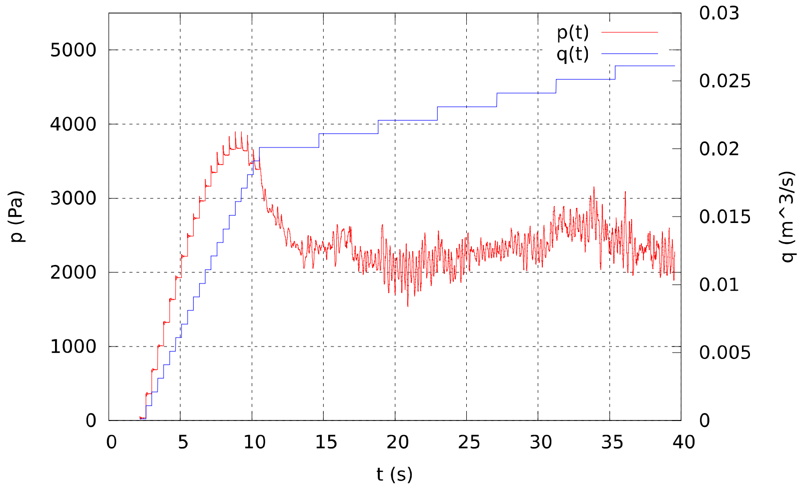

Figure 2. Evolution of the pressure in the time when the flow rate is increased from 0.0001 m^3/s, till 0.0261 m^3/s with increments of $0.001m^3/s$ (27 steps)

THE NUMERICAL RESULTS

The regimes

The numerical results obtained show a progressive development of a fluidized zone in a bed of grains, immersed in a liquid, under the effect of a localized upward flow injected at the bottom of the bed. It is seen that, gradually, by increasing the injected flux, four regimes are successively observed in the sample depending on the flow rate transiting through the injection point: (i.) Static regime: the granular layer remains immobile during the entire sequence with an imposed flow rate; (ii.) Dilatation regime: the sample dilates but does not develop a fluidized zone; (iii.) Cavity regime: a fluidization zone develops just above the injection point (Figure 3) and like a bubble, moves up and down along the central part of the sample but does not reach the top of the sample. Only the grains into the cavity are in movement; (iv.) Chimney regime: the fluidization zone quickly reaches the top of the sample thereby creating a chimney of fluidized grains

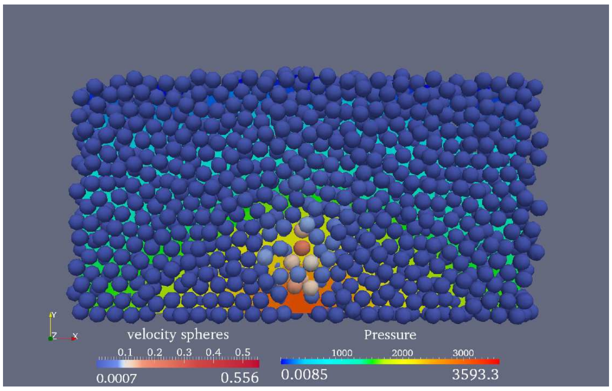

Figure 3. Development of the fluidized zone (t=13 s)

These regimes can be characterized by an estimation of the position, along the vertical axis, of the fluidized zone (height of the cavity). It will be zero in static regime and in dilatation regime, between zero and the height of the sample (*H*) in cavity regime and almost equal to *H* in chimney regime. Numerically, it is possible to represent the fluidized height in the time, through the highest position of the particles having a velocity higher than a threshold value (v_{lim}) opportunely chosen. The following graphs (Figures 4 and 5) show the evolution of the height of the cavity (h_f), of the height of the sample (*H*) and of the excess of pressure (*p*) for each injected flux step. These values correspond to average values over a given time period once the established regime has been reached. To discriminate the different regimes let us denote the following critical flow rate values: (i.) Q_{dil}: flow rate value from which there is a sample dilatation; (ii.) Q_{cav}: from this flow rate value the sample reaches the cavity regime ($h_f > 0$); (iii.) Q_{chim}: the height of the cavity reaches the height of the sample.

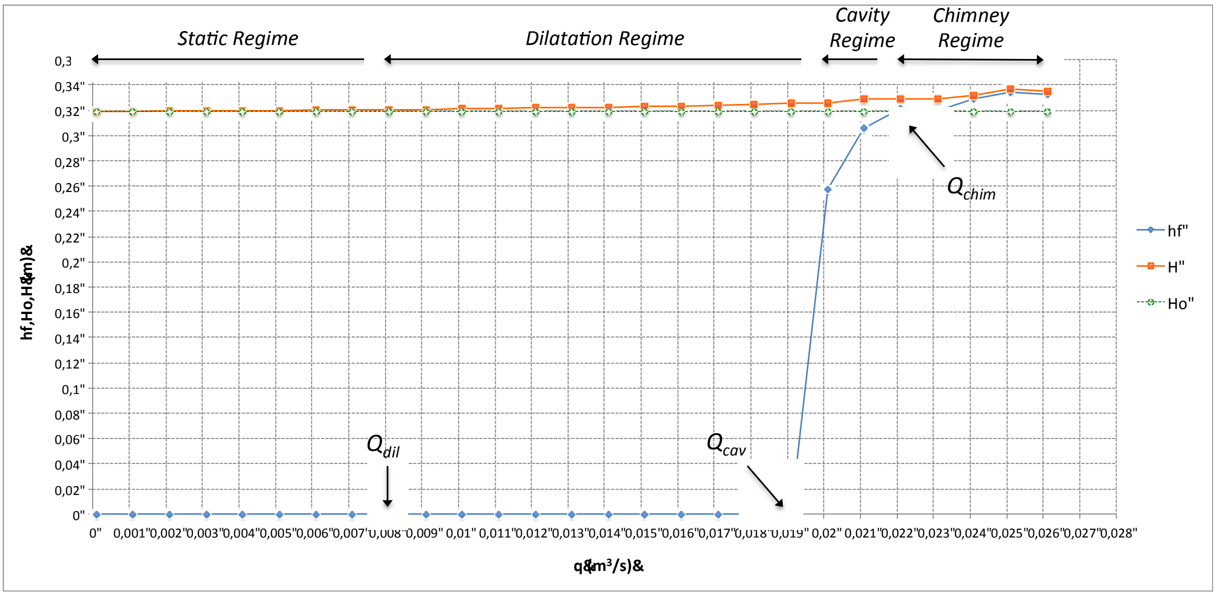

Figure 4. Evolution of the average value of the height of the cavity (h_f) and of the sample height (H) versus the injected flux (q) from 0.0001 m^3/s, till 0.0261 m^3/s

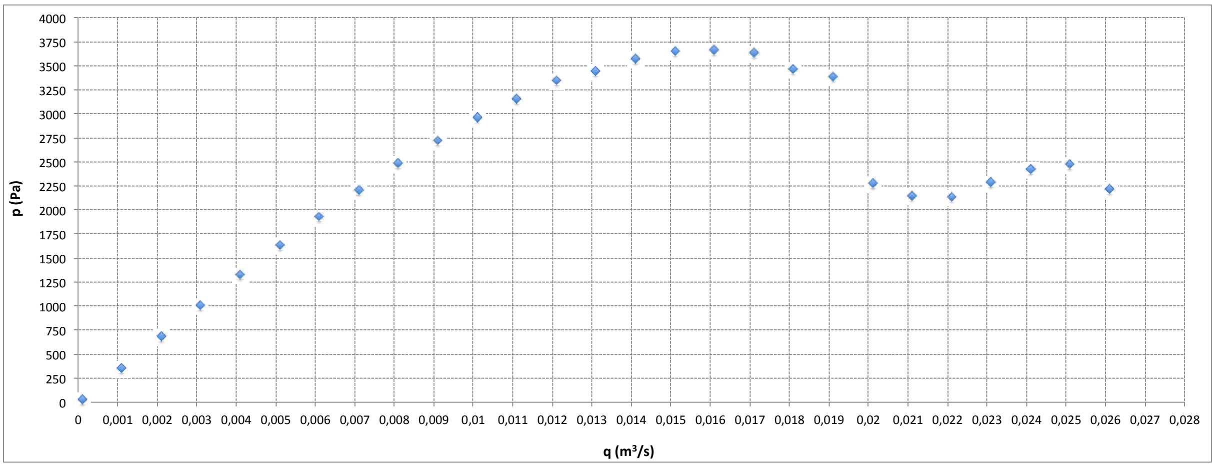

Figure 5. Evolution of the average value of the excess pressure (p) versus the injected flux (q) from 0.0001 m^3/s, till 0.0261 m^3/s

Interesting considerations can be done comparing the Figures 4 and 5. (i.) Static regime: for $0.0001 \leq q < 0.009$ m^3/s, the particles are statics and the pressure linearly grows with the flow. (ii.) Dilatation regime: for $0.009 \leq q \leq 0.016$ m^3/s, due to the decompression of the sample the pressure increases more slowly with increasing flow rate till a maximum value of 3671 Pa. It means that the hydraulic conductivity of the granular assembly, increase due to an increase of the porosity. For $0.016 < q < 0.019$ m^3/s the height of the sample increases more rapidly by increasing the flow rate causing an additional decompression of the sample; the pressure decreases until 3386 Pa. (iii.) Cavity regime: for $0.019 < q < 0.022$ m^3/s, with the formation of the fluidized zone the pressure drops quickly. (iv.) Chimney regime: for $q > 0.022$ m^3/s: when the fluidized zone reaches the top of the cavity, a convective motion is triggered, causes compression and decompression of the sample and consequently oscillatory pressure trend.

DIMENSIONLESS GRAPHS AND COMPARISON WITH THE EXPERIMENTAL RESULTS

Three samples (A,B,C) with different numbers of particles are considered (Table 2).

Table 2. Geometrical and mechanical characteristics of the samples A, B, and C

Characteristics of the samples				
		A	B	C
Width (w)	[m]	0.60	0.60	0.60
Height (H_0)	[m]	0.319	0.317	0.321
Depth (d)	[m]	0.10	0.10	0.10
N° spheres	[-]	2000	3000	4000
Mean diameter (d_m)	[m]	0.0225	0.0197	0.0179
Density of the solid phase (ρ_s)	[kg/m^3]	2600	2600	2600
Dynamic viscosity (μ)	[Pa.s]	0.01	0.01	0.01
Contact friction	[°]	10	10	10
Normal contact stiffness ($k_n/2r_m$)	[Pa]	400000	400000	400000
Ratio shear/normal stiffness (k_s/k_n)	[-]	0.5	0.5	0.5

For each sample, the injected flux is increased from an initial value of 0.0001 m^3/s till 0.0261 m^3/s with increments of 0.001m^3/s (27 steps), and the excess pressure in the middle of the bottom face of the sample is computed. Bigger is the number of the particles, smaller is their mean radius, smaller is the permeability of the sample; and bigger is the pressure computed at the bottom for a given value of injected flux. In the same way, the critical values the injected flux, for which the fluidized zone develops and reaches the top of the sample, are also different for the three specimens. By scaling the pressure, the flux and the height of the fluidized zone using respectively the coefficients α, β and δ, we define the following normalized parameters p/α, q/β, and h_f/δ.

$$\alpha = \rho_s \cdot g \cdot \frac{H_0^2}{D}\left[Pa\right]; \qquad \beta = \frac{\rho_s \cdot g \cdot H_0^2 \cdot D^2}{\mu}\left[\frac{m^3}{s}\right]; \qquad \delta = H_0\left[m\right].$$

Then two normalized graphs are plotted. The first (Figure 6) shows the evolution of the normalized excess of pressure (p/α) with the normalized flux (q/β). In this way it is possible to have ranges of normalized injected flux for which the four different regimes are observed: the static layer, the dilatation, the development of the fluidized cavity and the fluidization of the total height. The second dimensionless graph (Figure 7) shows the evolution of the normalized height of the cavity (h_f/δ) with the normalized flux (q/β) and permits to compare the numerical results obtained with the previous experimental ones conducted by Philippe and Badiane (2011, 2013), using a physical model. The scaled curves relatives to the numerical simulations of the samples A, B and C are not far from the scaled curve relative to the experimental results. The difference can be explained by the fact that the permeability of the numerical model may be slightly different from the one of the physical model (nothing has been done to tune the numerical permeability) leading to slightly different values of flux.

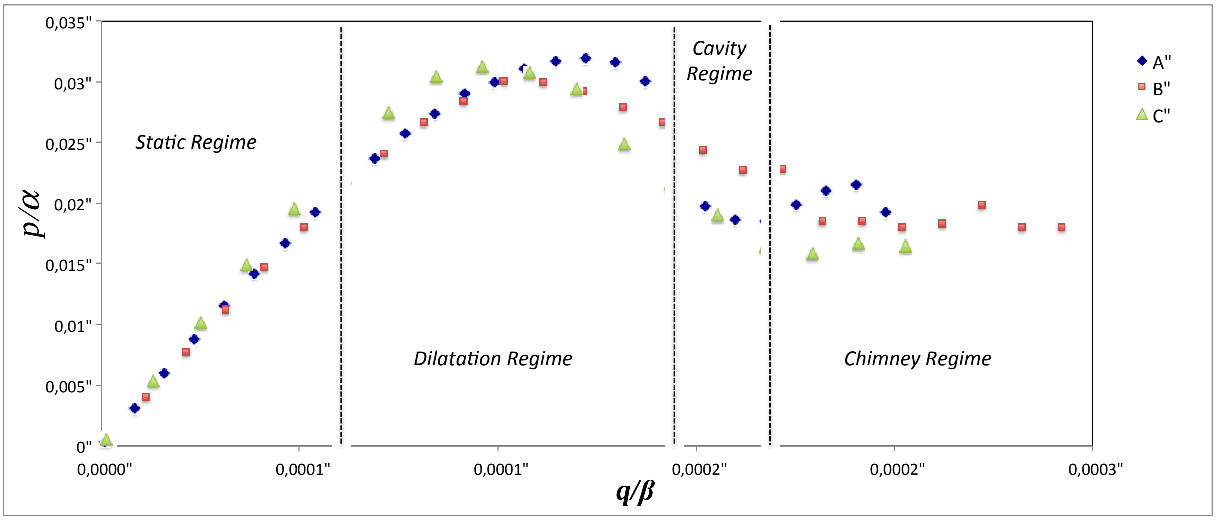

Figure 6. Evolution of the normalized excess of pressure (*p/α*) with the normalized flux (*q/β*)

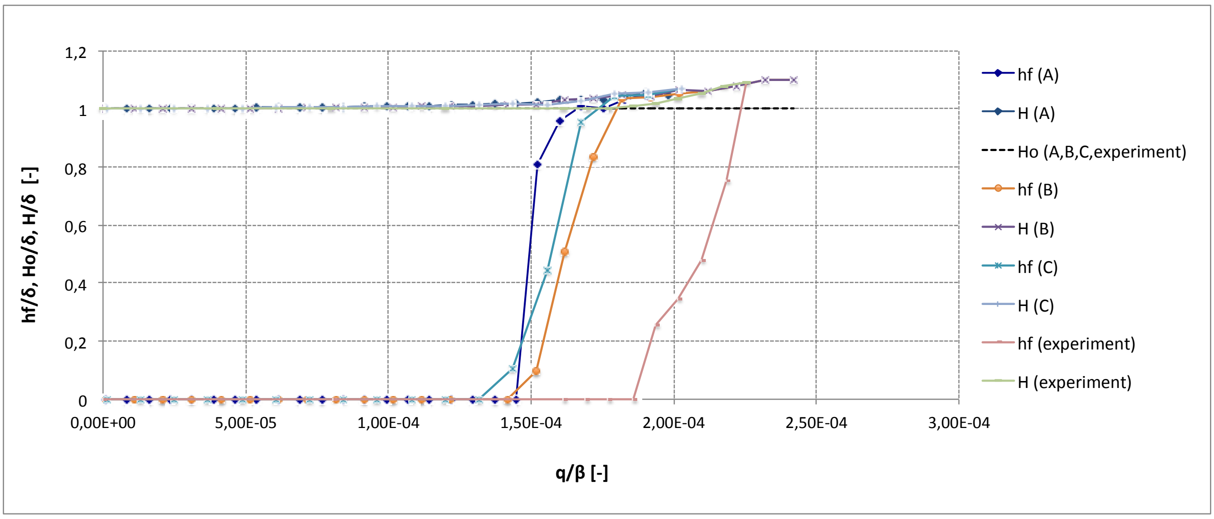

Figure 7. Evolution of the normalized height of the cavity (h_f/δ) with the normalized flux (q/β)

CONCLUSION

Numerical simulations of the localized fluidization in a saturated granular medium have been presented. The numerical results show the progressive development of different regimes inside the sample, depending on the increasing injected flux transiting through the injection point, in agreement with the experimental results. The qualitatively comparison of the phenomenon observed experimentally and simulated numerically is satisfactory; the comparison via dimensionless graph shows that the numerical results are not far from those obtained by Philippe and Badiane (2011, 2013) using a physical modelling. It means that the coupled model DEM-PFV used in this study, is able to simulate the phenomenon in object. However the work is not finished, more investigations are needed to better analyse quantitatively the problem using smaller particles, and computing stress and deformation in the sample. In addition, in the current configuration of the numerical model the size of the injection hole is dependent on the size of the particles. We think this particular configuration has an effect on the scaling of the parameters of the problem (such as the introduction of the size of the particles in the scaling of the pressure). This should be corrected by defining an injection hole independent of the particle size.

REFERENCES

P. Philippe and M. Badiane (2013). Localized fluidization in a granular medium. *Physical Review* E 87; DOI:10.1103/PhysRevE.87.042206

P. Philippe and M. Badiane (2011). Chimney of Fluidization and “Sandboil” in a Granular Soil. S. Bonelli et all (eds.), *Advances in Bifurcation and Degradation in Geomaterials* -Proceedings of the 9th International Workshop on Bifurcation and Degradation in Geomaterials- Springer Series in Geomechanics and Geoengineering 11: 125-129; DOI:10.1007/978-94-007-1421-2_16

E. Catalano, B. Chareyre and E. Barthélémy (2014). Pore-scale modeling of fluid-particles interaction and emerging poromechanical effects. *International Journal for Numerical and Analytical Methods in Geomechanics* 38:51–71; DOI: 10.1002/nag.2198

H. Sari, B. Chareyre, E. Catalano, P. Philippe and E. Vincens (2011). Investigation of internal erosion processes using a coupled DEM-fluid method. *II International Conference on Particle-based Methods* – Fundamentals and Applications PARTICLES 2011 E. Oñate and D.R.J. Owen (Eds.)

A.-T. Tong, E. Catalano and B. Chareyre (2012). Pore-Scale Flow Simulations: Model Predictions Compared with Experiments on Bi-Dispersed Granular Assemblies. *Oil & Gas Science and Technology* – Rev. IFP Energies nouvelles 67(5):743-752; DOI: 10.2516/ogst/2012032